Materials and Design 147 (2018) 167–174

Contents lists available at ScienceDirect

Materials and Design

journal homepage: www.elsevier.com/locate/matdes

Surfactant-aided impregnation of MnF_2 into CNT fabrics as cathode material with high electrochemical performance for lithium ion batteries

Nasr Bensalah [a,*], Dorra Turki [a], Khaled Saoud [b]

[a] Department of Chemistry and Earth Sciences, College of Arts and Sciences, Qatar University, PO Box 2713, Doha, Qatar
[b] Virginia Commonwealth University in Qatar, PO Box 8095, Al Luqta Street, Education City, Doha, Qatar

HIGHLIGHTS

- Surfactant-aided impregnation of $MnSiF_6$ into CNT fabrics followed by annealing at 400 °C forms CNT-MnF_2 composites.
- Flexible CNT-MnF_2 cathodes retained a specific charge capacity of 388 mAh/g in half-cell after 100 cycles at 0.1 C.
- MnF_2 loading affects largely the capacity of CNT-MnF_2 and MnF_2 loading between 70% and 80% gives highest specific capacity.

GRAPHICAL ABSTRACT

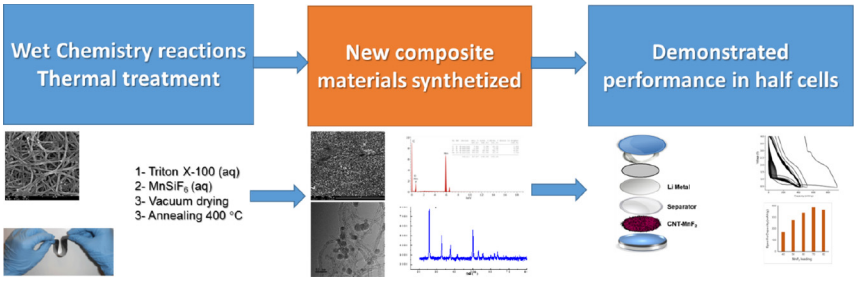

ARTICLE INFO

Article history:
Received 17 December 2017
Received in revised form 16 March 2018
Accepted 18 March 2018
Available online 19 March 2018

Keywords:
CNT fabric
Transition metal fluoride
Nanocomposites
Cathode material
Li ion battery

ABSTRACT

MnF_2 infiltrated-CNT fabrics was prepared by surfactant-aided impregnation of $MnSiF_6$ precursors in acid-treated CNT fabric followed by annealing $MnSiF_6$-loaded CNT fabric. The structural and morphological characterizations by X-ray diffraction, scanning electron microscopy (SEM), and transmission electron microscopy (TEM) confirmed the formation of MnF_2 nanoparticles (average size: 20–30 nm) within CNT fabric structure. Galvanostatic charge-discharge tests of CNT-MnF_2 nanocomposite fabrics showed excellent electrochemical performance and good cycle stability between 0.4 and 4.0 V vs Li/Li^+. A specific capacity of 388 mAh/g was measured at 0.1C for CNT-MnF_2 fabric with 70% MnF_2 loading after 100 cycles. Stable cyclability and good rate performance were obtained at high charge-discharge cycling rates. MnF_2 loading largely affect the performance of MnF_2 infiltrated-CNT fabrics cathodes when lower than 70% MnF_2 loaded-CNT fabrics were prepared. It can be concluded that nano-sized active materials infiltrated inside conductive carbon matrix in optimized content can lead to rapid kinetics and stable performance for flexible metal fluoride-based cathode materials.

1. Introduction

The demands for electrochemical energy storage devices including batteries, supercapacitors, and fuel cells are continuously increasing because of their expanded utilizations in portable electronic devices such as mobile phones, laptops, tablets, cameras, sensors, medical devices, etc. Li ion batteries (LIBs) are considered as excellent electrochemical storage devices due to their high energy density, long cycling lifetime, low self-discharge and resistance [1]. However, future applications in electric vehicles and renewable energy and backup power applications for off-grid or smart grid require batteries with high capacity, rugged durability, long life, reliable performance, safety, among others [1].

Intensive research efforts have been focused on the improvement of insertion/extraction kinetics of conventional cathode materials, i.e. transition metal oxides $LiMO_2$ and phosphates $LiMPO_4$ (M = Fe, Co, Mn, Ni, etc.) through nanostructuring to shorten Li^+ diffusion distance [1–3]. Although good results have been obtained related to cyclability and rate performance, these materials suffer from low Li^+ storage and limited specific energies. With the actual electrochemical properties,

* Corresponding author.
E-mail address: nasr.bensalah@qu.edu.qa (N. Bensalah).

https://doi.org/10.1016/j.matdes.2018.03.045
0264-1275/

layered transition metal oxide and phosphates cathodes cannot meet the new requirements for LIBs to continue being used in modern electronic devices, electric automobiles, and smart electricity grid. Nonetheless, LIBs will remain the principle electrochemical storage devices for years to come owing to the big progress in the development of advanced cathode materials capable to store more than one Li^+ ion or exchange more than one electron per molecular formula unit. These cathode materials undergo conversion/displacement reactions instead of insertion/extraction mechanisms during discharge/charge of the electrochemical cell.

Recently, transition-metal fluorides (TMFs) have been used as cathode materials in LIBs, and achieved high capacities and high energy densities [3–20]. The oxidation state of the metal in TMFs involves the transfer of multiple electrons/lithium ions per formula unit leading to higher theoretical volumetric capacity (up to ≈2200 mAh/cm^3) and higher theoretical potential (up to ≈3.5 V vs Li/Li^+). However, TMFs materials suffer from several shortcomings, which limit their stability. The most challenging one is the large volume and microstructural changes during insertion and extraction of Li. As a result, the stability of the investigated electrodes has been quite limited even in half cells. During charge/discharge, a displacement/conversion process takes place, where Li displaces the transition metal, leading to the formation of LiF and transition metal clusters. Due to the small diffusion distances between these thermodynamically stable structures, reversible Li insertion and extraction becomes feasible. Theoretically, the Li capacity of fluorides is determined by its stoichiometry and the density of the fluoride-forming metal according to (Fig. 1):

$$x\,Li^+ + x\,e^- + MF_x \leftrightarrows x\,LiF + M$$

where M is a fluoride-forming metal.

The low electrical conductivity of fluorides initially resulted in the low utilization of their theoretical capacity. However, reduction in the grain size of poor conductive materials and the incorporation of these nano-sized grains into a conductive matrix of carbon or even selected metal oxides [14,15,21–24] allowed significant enhancements of the cathode utilization (some close to the theoretical capacity). In an ideal case, such matrices should offer both electronic and ionic conductivities. Among the high voltage TMFs cathodes, some of the highest theoretical energy densities are exhibited by MnF_2 ((1519 Wh/kg; 577 mAh/g) [12,19].

Recently, several attempts to prepare nano-sized metal fluorides using pyrolysis, precipitation and supercritical-fluid technologies showed poor electrochemical performance after few cycles due to the inhomogeneity of structure and the composition [11–16,25–29]. More recently, Wang et al. [30] have demonstrated that the incorporation of CoF_2 nanoparticles inside CNTs fabric prepared *in situ* by annealing of CNT-$CoSiF_6$ composites enhanced the capacity of Li-ion batteries; however the capacity did not reach the theoretical value. From these results, it can be concluded that the morphology of the conductive carbon additives used in electrode fabrication determines the ability of metal fluoride cathode to retain capacity during conversion reaction with lithium. A deep understanding of the reaction mechanisms during charge/discharge of fluoride-based cathodes is desired to suppress the capacity fading and voltage decay of carbon-metal fluoride nanocomposites Li-ion cathodes. It is predicted that further improvement in electrochemical performance of carbon-metal fluoride cathodes can be obtained by carefully choosing the preparation method and the cycling voltages. Furthermore, we noticed that competitive insertion/extraction, and conversion/displacement mechanisms contribute in capacity fading of metal fluoride-based cathodes.

In this work, a simple method of preparation of MnF_2 infiltrated-CNT fabrics cathode material was developed. MnF_2 nanoparticles were incorporated inside the pores of carbon matrix by impregnation of CNTs fabric in $MnSiF_6$-H_2SiF_6 aqueous solutions in presence of Triton X-100 followed by vacuum drying at 80 °C and then annealing under argon atmosphere at 400 °C. The as-prepared CNT-MnF_2 fabric was studied in half-cell Li-ion batteries with pure Li metal as anode. The main goal of this work is to achieve significantly better performance of TMFs cathodes with nanostructured multi-component systems, where MnF_2 and CNTs offer synergetic performance enhancement by effectively mitigating the failure of both materials due to the exceptional mechanical properties of CNTs fabrics. Additionally, the design of lightweight, flexible and high-performance energy storage carbon-based materials becomes highly urgent to encounter the needs for portable and wearable electronic devices.

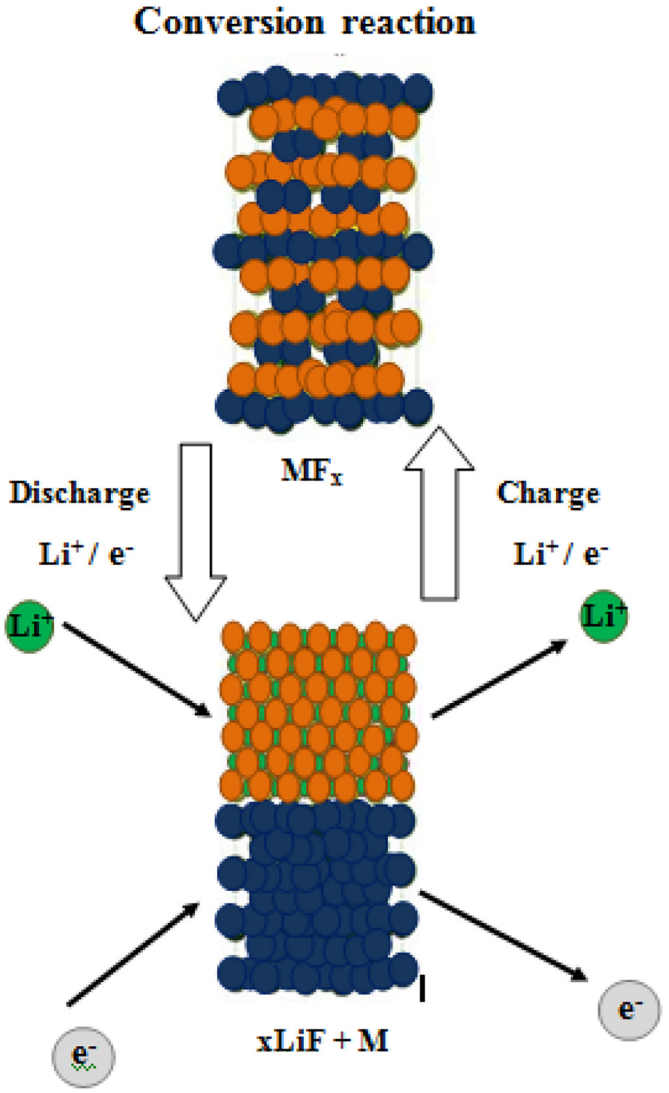

Fig. 1. Schematic of a reversible conversion reaction, showing crystallographic changes occurring during discharge and charge of a metal fluoride cathode.

2. Experimental

2.1. Chemicals

High purity manganese (Mn) power was purchased from Sigma Aldrich. Aqueous solution of fluorosilicic acid, H_2SiF_6 (20–25% weight) used as fluorinating agent was also purchased from Sigma Aldrich. Organic carbonates (dimethylene carbonate, diethylene carbonate, and ethylene carbonate) were of analytical grade and obtained from Sigma Aldrich. Li ribbon (thickness × width 0.75 mm × 100 mm, 99.9% trace metals basis) from Sigma Aldrich was used as anode material. Lithium hexafluorophosphate $LiPF_6$ (battery grade, ≥99.99% trace metals basis)

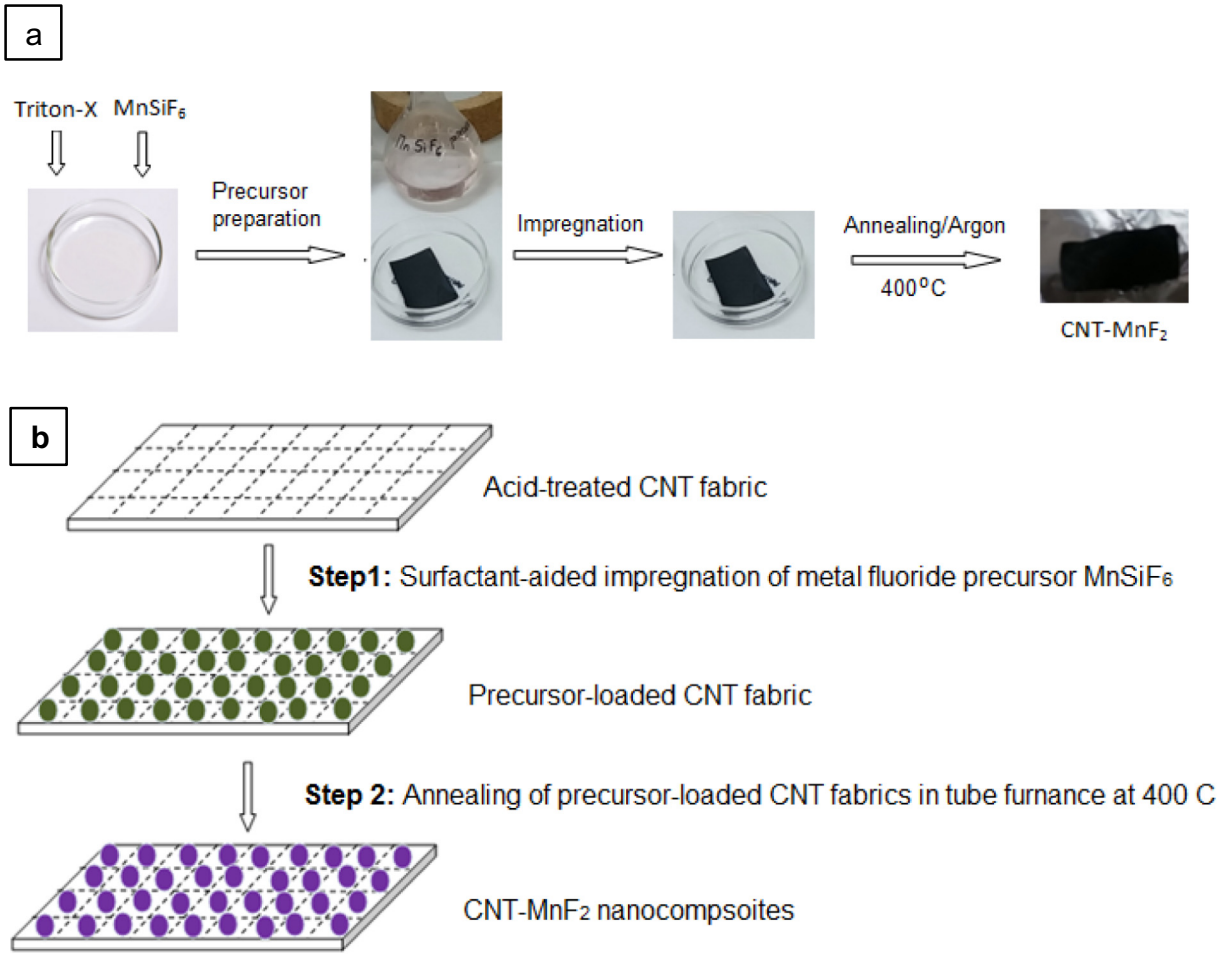

Fig. 2. a) Experimental steps, b) Simple scheme of the synthesis of CNT-MnF_2 nanocomposite fabrics.

product of Aldrich was used as supporting electrolyte. The surfactant of Triton X-100 was purchased from VWR.

2.2. Preparation of manganese(II) hexaflurorosilicate $MnSiF_6$

$MnSiF_6$ was prepared by chemical reaction of manganese metal with fluorosilicic acid according to the following reaction: $Mn(s) + H_2SiF_6(aq) \rightarrow MnSiF_6(aq) + H_2(g)$. 3 g Mn powder was slowly added to 50 mL H_2SiF_6 aqueous solution. The mixture was kept under magnetic stirring during 12 h till all the manganese was dissolved. The pink clear aqueous solution was sealed and kept in refrigerator at 4 °C in Teflon bottle until utilization.

2.3. Pretreatment of carbon nanotubes (CNT) fabrics

The carbon nanotubes (CNT) fabrics were produced by floating catalyst chemical vapor deposition FCCVD using ethanol as the primary carbon source and ferrocene as the source for iron catalyst. CNTs fabrics were soaked in 6 M HNO_3 for 12 h to enhance its wettability and remove metallic and polymeric impurities. It is washed with water till neutral pH, and then several times with acetone. After drying at 70 °C in vacuum oven, the acid-treated CNT fabrics were thermally treated at 550 °C in furnace tube during 6 h under Argon atmosphere.

2.4. Preparation of CNT-MnF_2 nanocomposites

10 mL of $MnSiF_6$ was mixed with 4.5 mL 0.1% triton X-100 aqueous solution. A desired mL of this solution was introduced in a petri dish. CNT fabric of 5 cm^2 area was immersed into the solution and left till complete impregnation of the precursor solution inside the carbon matrix was obtained. $MnSiF_6$-loaded CNT material was dried at 70 °C under vacuum and then annealed at 400 °C in furnace tube under Argon atmosphere for 4 h to completely decompose $MnSiF_6$ and obtain MnF_2 nanoparticles infiltrated inside CNT fabric structure according to the equation: $MnSiF_6(s) \rightarrow MnF_2(s) + SiF_4(g)$. SiF_4 gas was captured by

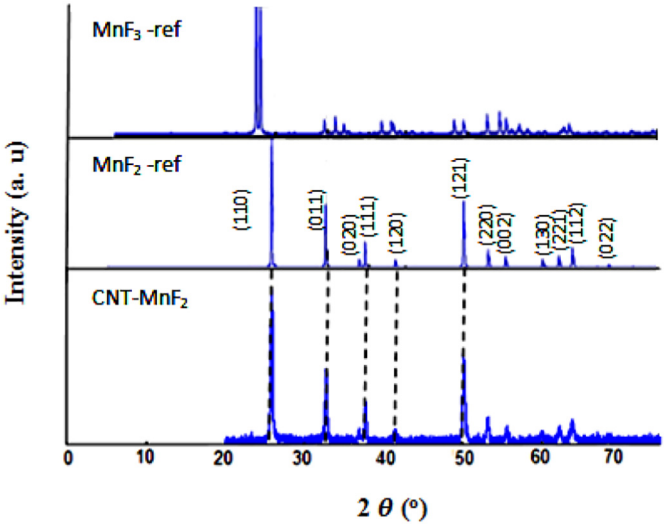

Fig. 3. XRD patterns of MnF_2 particles deposited on the surface on CNT-MnF_2 nanocomposite fabric with 70% MnF_2 loading, and MnF_2 and MnF_3 powders.

sparging the gas in 10 M KOH aqueous solution. The loading of MnF_2 in the CNT-MnF_2 nanocomposite can be increased by soaking the treated CNT fabric in more concentrated precursor solution. The loading of MnF_2 deposited onto CNT fabrics in the different CNT-MnF_2 composites ranges from 1.8 mg/cm^2 to 3.5 mg/cm^2.

2.5. Characterization of MnF_2 infiltrated_CNT fabrics

The crystal structure of MnF_2-infiltrated CNT fabric was characterized by powder X-ray diffraction (XRD; Rigaku Ultima IV, 40 kV/30 mA, Cu-K_α radiation) at a scan rate of 2°/min with a diffraction angle 2θ between 10° and 80°. The morphology of synthesized samples was observed by Scanning Electron Microscopy (SEM, JEOL JSM-6610) and Transmission Electron Microscopy (TEM JEOL JEM-2100F). The content of MnF_2 in the composite was determined by mass difference before and after annealing using microbalance (Mettler Toledo™ Excellence Plus, XPE Series).

2.6. Electrochemical tests

The electrochemical tests of MnF_2-CNT nanomaterials were performed in CR2032 coin cells. The prepared MnF_2/CNTs nanocomposite was directly cut into disks and assembled inside Argon-filled glove box (MTI, with gas purification system and digital Control - EQ-VGB-6-LD) with an oxygen and water content <0.1 ppm using Li metal disks as the counter and reference electrodes and a polypropylene membrane (Celgard, 2500) as a separator. 1 M $LiPF_6$ dissolved in 1:1:1 (v/v/v%) EC/DMC/DEC solvents was used as electrolyte. Galvanostatic charge-discharge tests of Li/MnF_2-CNT batteries were conducted using MTI 8 channel battery analyzer (BST8-WA, 0.005–1 mA, up to 5 V) with adjustable cell holders in the voltage range 0.4–4.0 V at various rates. Cyclic voltammetry (CV) and electrochemical impedance spectroscopy (EIS) were performed on cells using a potentiostat/galvanostat (Model PGSTAT302N, MetrohmAutolab) running Nova software. The impedance was carried out in potentiostatic mode at open-circuit potentials at a fully

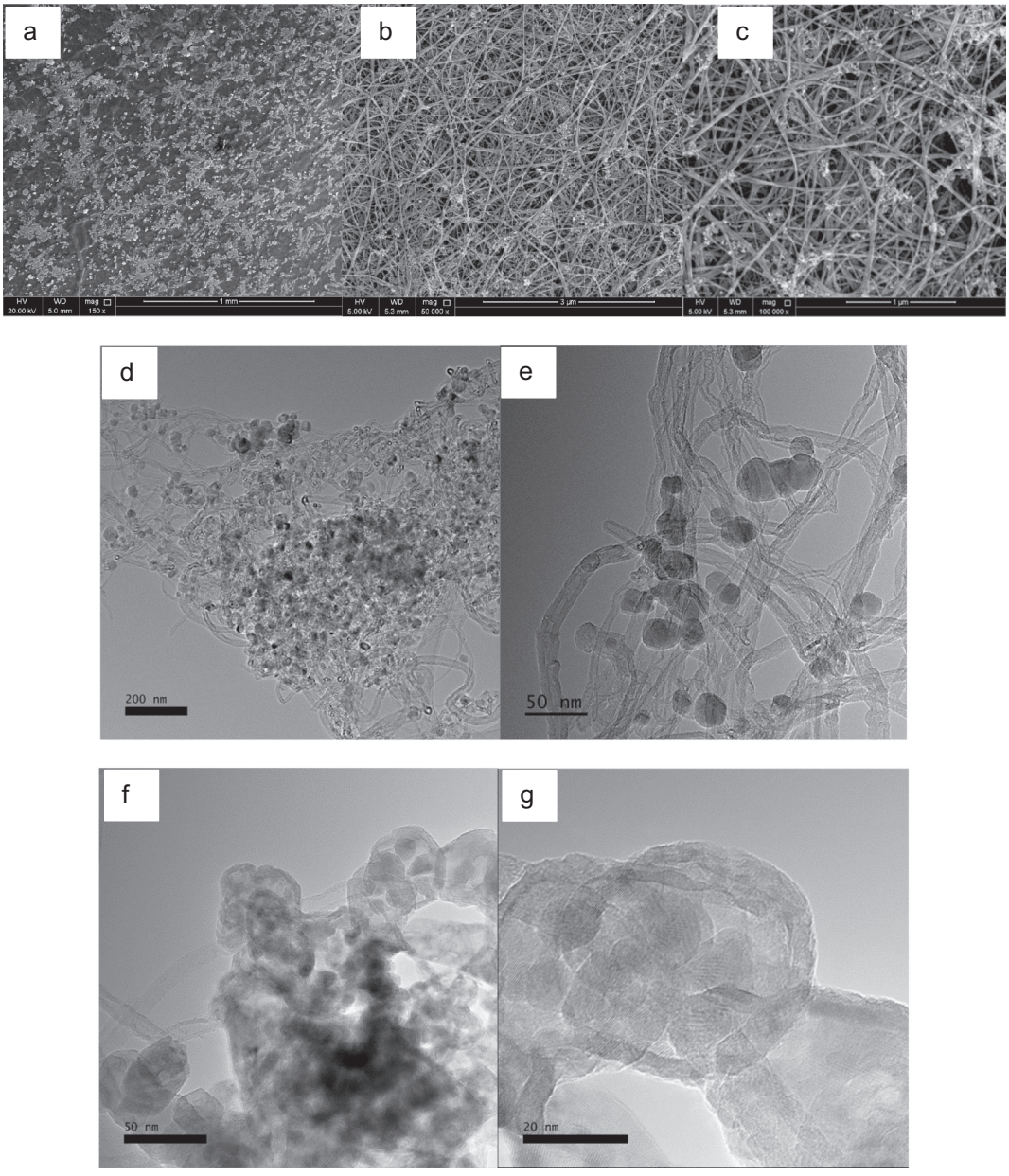

Fig. 4. Morphology characteristics of CNT-MnF_2 nanocomposite fabric with 70% MnF_2 loading: a–c) SEM image of nanocomposite surface at different magnifications; d–g) TEM photos of the MnF_2-loaded CNTs taken from the surface of CNT-MnF_2 fabric by high frequency ultrasound and dispersed in acetone.

charged state. The amplitude of the AC signal was set at 5 mV and the frequency ranged from 1 MHz to 10 MHz.

3. Results and discussions

Fig. 2 illustrates all the steps of formation of MnF_2 nanoparticles infiltrated inside CNT fabrics. MnF_2-CNT cathodes were prepared based on a modified method used by Wang et al. [30] to prepare CoF_2-CNT nanomaterials. The modification was opted to improve the wettability of initially hydrophobic CNTs fabrics, to increase the metal fluoride loading inside CNTs microstructure, and to strengthen the interconnections between MnF_2 nanoparticles and the CNT supporting material. The precursor $MnSiF_6$ was firstly impregnated inside the acid-treated CNT fabric by soaking CNT fabrics in $MnSiF_6$ 0.1% triton aqueous solution. The solution was completely absorbed by the acid-treated CNT fabrics. The impregnation was aided by triton X-100 surfactant to further lessen hydrophobic properties of treated CNT fabrics and ensure a well distribution of the precursor within CNT structure. The formation of MnF_2 nanoparticles occurred by annealing the vacuum dried $MnSiF_6$ loaded CNT fabric at 400 °C for 4 h. Under these thermal conditions, $MnSiF_6$ would be decomposed completely into MnF_2 and SiF_4 and triton X-100 would be also carbonized.

XRD spectra of synthetized CNT-MnF_2 nanocomposites, MnF_2 and MnF_3 are given in Fig. 3. These results depict the coincidence of the peaks of the synthetized materials with those of pure MnF_2 power. It is obvious that the synthesis method results in the formation of MnF_2 particles on the surface of CNT fabric and incorporated inside its structure. This result confirms that the oxidation state of manganese does not change during annealing step by thermal decomposition of $MnSiF_6$. Similar results have been reported in literature with other transition metal fluorides such as FeF_2 and CoF_2 [26,30]. SEM graphs of CNT-MnF_2 nanocomposites given in Fig. 4-a-c at different magnifications, shows that MnF_2 particles are well distributed on the surface of CNT fabric. In addition, it is clear that MnF_2 particles are infiltrated inside the structure of CNT fabric and the crystal particles are precipitated on the voids and on the surface of carbon matrix. TEM images of the nanomaterials taken by high frequency sonication and dispersed in acetone showed that the average size of MnF_2 nanoparticles is estimated to be between 20 and 30 nm as shown in Fig. 4-d-g. In addition, Fig. 4-g shows the lattice fringes indicating an oriented growth of MnF_2 nanocrystals. EDS elemental analysis shown in Fig. 5 confirms the presence of Mn and F elements in the composition of MnF_2 precipitate. It is well documented that the size of active materials and interfacial interactions between the active materials and the supporting material are equally essential to determine the performance of conversion-type Li-ion batteries. Therefore, the impregnation of $MnSiF_6$ inside CNT fabrics resulted in the precipitation of nanoscaled and porous active MnF_2 within the structure of flexible and conductive carbon matrix.

Electrochemical behavior of the CNT-MnF_2 samples was firstly studied using cyclic voltammetry (CV) in half-cells with Li metal counter electrodes between 0.4 and 4.0 V (Fig. 6-a). CNT-MnF_2 composites showed an electrochemical activity within voltage window. In the first cycle, two oxidation peaks appeared at 2.15 and 2.75 V vs Li/Li^+ corresponding to the electrochemical oxidation of Mn^{2+} to higher oxidation states and the decomposition of electrolyte with formation of SEI. In the return cycle, a reduction peak appeared around 1.0 V corresponding to the reduction of Mn^{2+} into Mn. It is markedly noted from the results of Fig. 6-a that the electrochemical behavior changed after the first

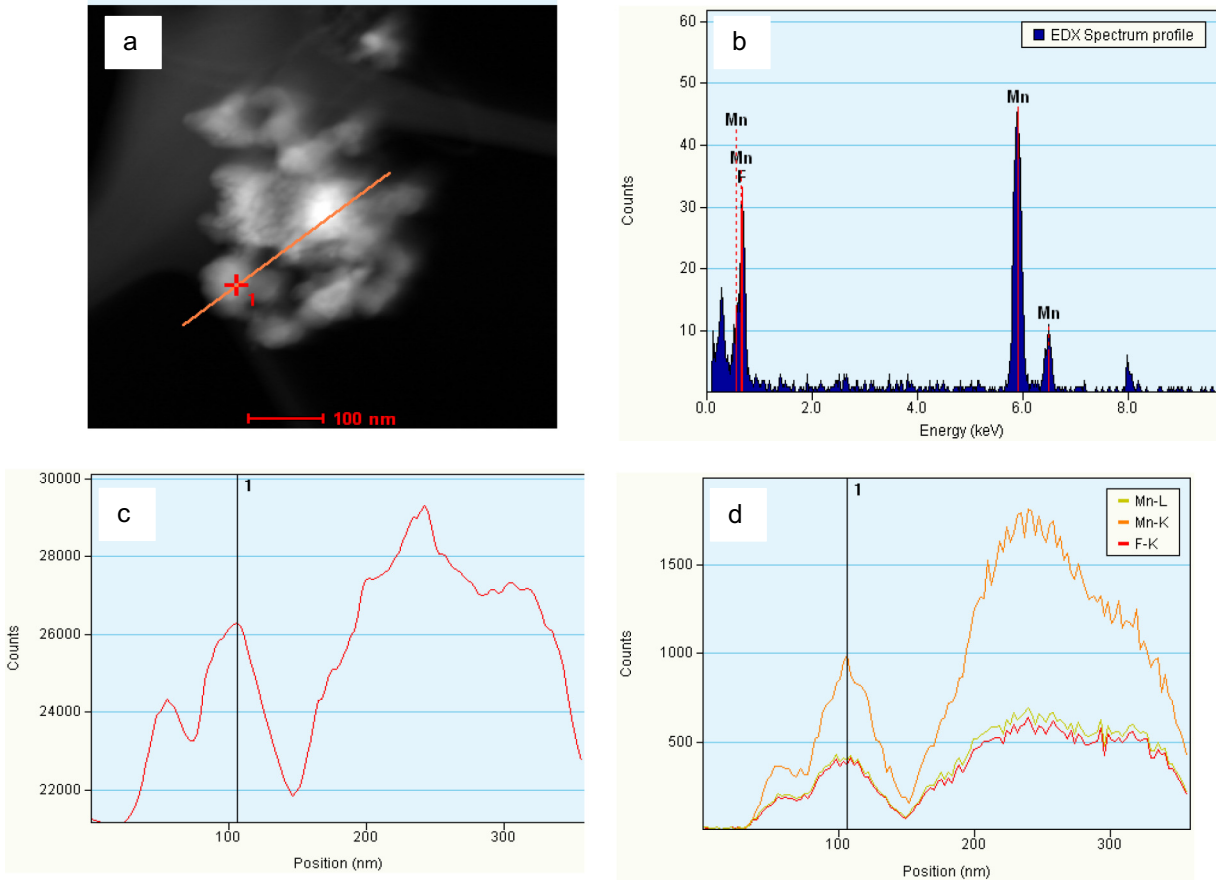

Fig. 5. TEM EDX analysis of MnF_2-loaded CNTs taken from the surface of CNT-MnF_2 fabric with 70% MnF_2 loading by high frequency ultrasound and dispersed in acetone (a) STEM-HAADF image of MnF_2 nanoparticle, (b) EDX analysis of the particle on the position (x) in a) showing that the nanoparticle was composed of mainly Mn and F, (c) Distribution of all the elements, and (d) Distribution of Mn and F along the entire orange line in a).

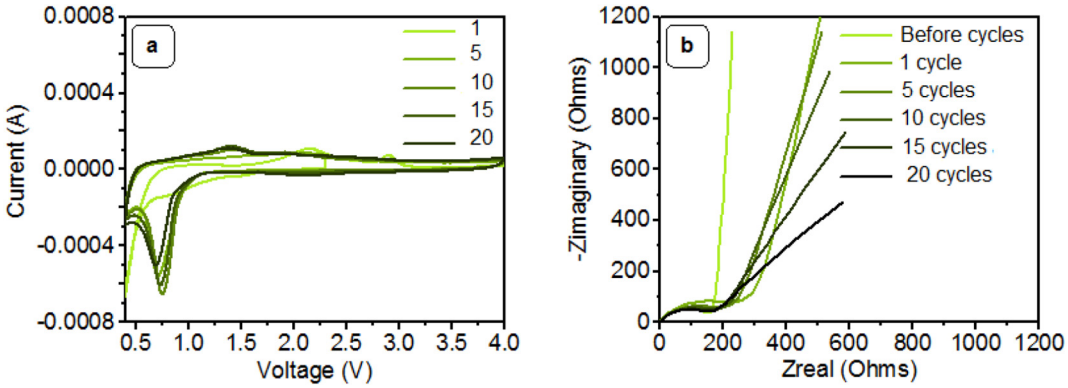

Fig. 6. (a) Cyclic voltammograms, and (b) EIS of CNT-MnF_2 samples tested with 1 M $LiPF_6$ dissolved in 1:1:1 (v/v/v%) EC/DMC/DEC electrolyte in Li metal half-cells and 0.3 mV s^{-1} scan rate.

cycle and only two peaks appeared in the CV; an oxidation peak at 1.42 V vs Li/Li^+ and a large reduction peak at 0.75 V vs Li/Li^+. These peaks correspond to the main conversion charge and discharge reactions of electrochemical oxidation of Mn metal into MnF_2 and liberation of Li^+ and electrochemical reduction of MnF_2 into Mn with formation of LiF. The difference between the oxidation and reduction potentials suggested a slow kinetics for the conversion reactions; however, a very stable performance for CNT-MnF_2 electrode appeared during successive cycling.

Electrochemical impedance spectroscopy was also performed before and after CV cycles (Fig. 6-b). The electrical resistance, indicated by the magnitude of the horizontal axis intercept, was low and did not change much during cycling (~2 Ω). Also, the charge-transfer resistance, determined from the radius of the semicircular feature present in the plot (150 Ω before cycling), was reasonably small. The charge-transfer resistance increased after cycling and then it returns to its initial value after cycle 5 which may be due to the formation of SEI. This result indicates that the electrodes are well electrically connected and have sufficient channels for ion flow (solid state through the particles and through the electrolyte).

The electrochemical performance of CNT-MnF_2 nanocomposites as cathode materials in half-cell configuration using Li metal as counter and reference electrode was also evaluated using galvanostatic charge-discharge tests. The open circuit potential of Li/CNT-MnF_2 battery was 3.2 V vs Li^+/Li. The galvanostatic charge-discharge tests were performed in the voltage range 0.4 to 4.0 V vs Li^+/Li at room temperature 23–24 °C. Fig. 7-a presents the charge-discharge cycles against capacity (mAh/g MnF_2) of CNT-MnF_2 nanocomposites (70% MnF_2 in mass) at 0.1 C in respect of the theoretical capacity of MnF_2 active materials 577 mAh/g. With lower voltage limit (0.4 V vs Li/Li^+), we obtained capacities for CNT-MnF_2 of roughly 400 mAh/g at the peak. As it can be seen from Fig. 7, charge-discharge plateaus appeared and the insertion of Li occurs ~1 V vs. Li/Li^+. This indicates that CNT-MnF_2 cycled at lower voltage than 1.0 V gives better performance and more stability to the electrochemical cells. A specific discharge and charge capacities of 924 mAh/g and 460 mAh/g were measured with a coulombic efficiency around 200% indicating the irreversibility of the electrochemical reactions in the first cycle. The specific discharge capacity was surprisingly higher than the theoretical specific capacity for MnF_2 (577 mAh/g). Higher discharge specific capacity than the theoretical value for CNT-MnF2 cathode and irreversible specific capacity in the first cycle can be linked to the side reactions of the electrolyte and the formation of the SEI film.

After 100 cycles, a charge specific capacity of 388 mAh/g was measured for CNT-MnF_2, which represents 84% the initial specific charge capacity measured (Fig. 7-b). CNT-MnF_2 nanocomposites cathode displayed CE values very close to 100% in long cycles, indicating the high reversibility of electrochemical conversion reactions. It seems that the joint assembly between the flexible and conductive CNT fabric facilitates the charge transfer and absorbs the volumetric changes during conversion reactions [21–30], which maintains the specific capacity of CNT-MnF_2 cathodes during charge-discharge cycles. The measured specific capacity, 388 mAh/g, was about 67% the theoretical capacity of pure MnF_2 material (577 mAh/g). This can be due to incomplete charge-discharge reactions limited by cycling voltage loop fixed to be between 0.4 and 4.0 V vs. Li^+/Li to minimize electrolyte degradation

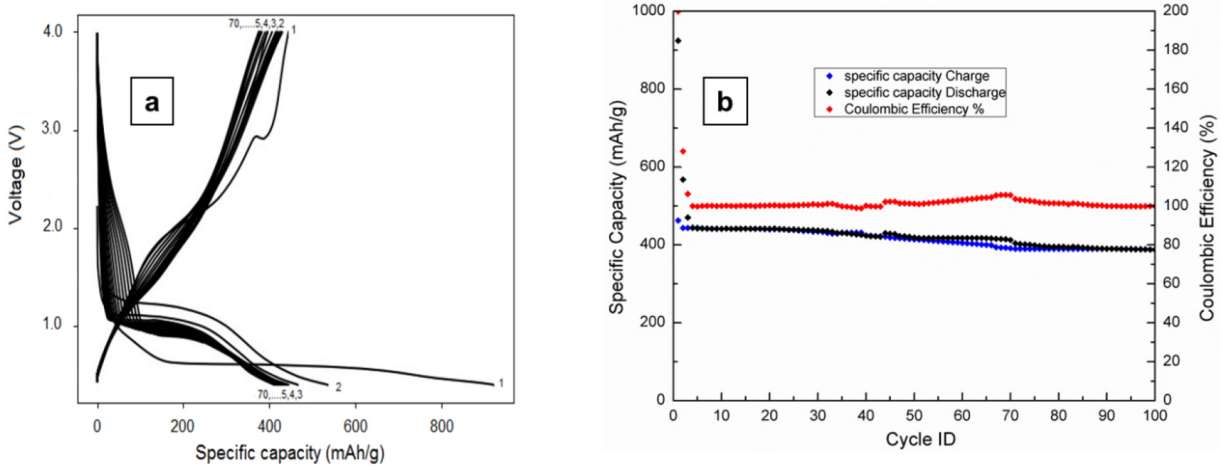

Fig. 7. Electrochemical performance and stability of CNT-MnF_2 nanocomposite fabric with 70% MnF_2 loading: a) Voltage vs capacity for 100 first cycles between 0.4 and 4.0 V at 0.1 C; b) capacity and coulombic efficiency vs cycle ID for 100 first cycles. Experimental Conditions: 1 M $LiPF_6$ dissolved in 1:1:1 (v/v/v%) EC/DMC/DEC electrolyte in Li metal half-cells.

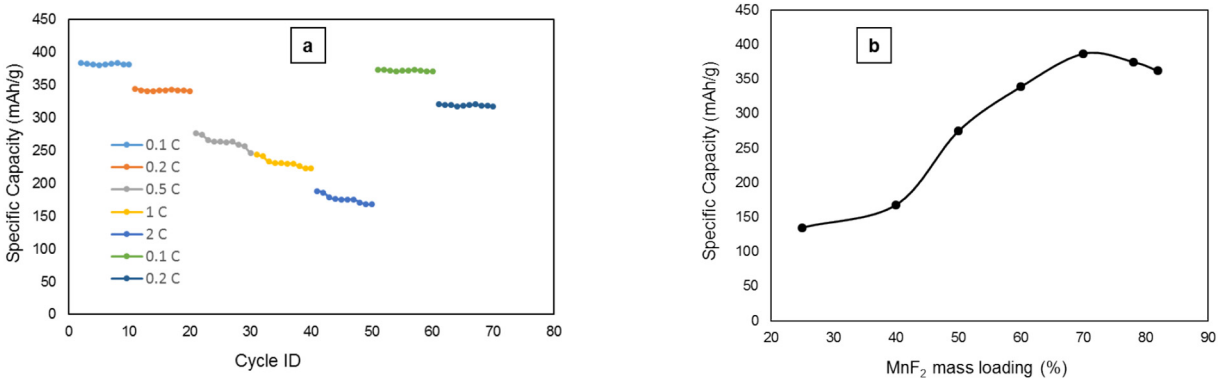

Fig. 8. Electrochemical properties of CNT-MnF_2 nanocomposite fabrics: a) Effect of cycling rate on specific capacity vs cycle ID during galvanostatic charge-discharge cycling of CNT-MnF_2 nanocomposite fabric with 70% MnF_2 loading; b) Effect of MnF_2 mass loading on discharge capacity of CNT-MnF_2 nanocomposite fabric. Experimental Conditions: 1 M $LiPF_6$ dissolved in 1:1:1 (v/v/v%) EC/DMC/DEC electrolyte in Li metal half-cells.

and by the slowness of conversion reactions. In contrast to previously reported results [11,25–30] related to metal transition fluorides, our results demonstrated a good electrochemical stability of CNT-MnF_2 nanocomposites cathodes. The excellent electrochemical properties of CNT-MnF_2 nanocomposites as cathode material for Li-ion batteries suggests that the infiltration of MnF_2 nanoparticles inside CNT structure accelerates charge and Li ions transfer during charge-discharge cycles by keeping a good connectivity and an unceasing electrical contact between the conductive CNT support and the weakly-conductive active MnF_2 nanomaterials which results in high capacity and durable cyclability.

CNT-MnF_2 nanocomposites cathodes were continuously tested at different charge-discharge rates (after 100 cycles at 0.1 C) for 10 first cycles as shown in Fig. 8-a. The composite cathodes materials showed initial capacities of 388 mAh/g at 0.1 C, 345 mAh/g at 0.2 C, 277 mAh/g at 0.5 C, 244 mAh/g at 1 C, 188 mAh/g at 2 C, and 108 mAh/g at 5 C. CNT-MnF_2 nanocomposites showed a remarkable capacity retention of 97% and 93% after recycled again at 0.1 C and 0.2 C. MnF_2 loading inside the structure of CNT fabrics would affect the electrochemical performance of CNT-MnF_2 cathode materials. The discharge capacity of different loaded CNT-MnF_2 at 0.1 C given in Fig. 8-b showed that increasing MnF_2 loading up to 70% in weight increased the capacity from 135 mAh/g at 25%, to 168 mAh/g at 40%, to 275 mAh/g at 50%, to 340 mAh/g at 60%, and to 388 mAh/g at 70%. However, increasing MnF_2 loading >70% decreased the capacity to 375 mAh/g at 78% and 362 mAh/g at 82%. It is obvious that a MnF_2 loading between 70 and 80% resulted in higher specific capacity and more stable performance of CNT-MnF_2 nanocomposites cathodes. This suggests that the amount of MnF_2 active materials and the interconnectivity inside the carbon matrix are major factors in determining the performance of CNT-MnF_2 nanocomposites. The greater lithium storage capability of CNT-MnF_2 cathodes is related to the amount of nano-sized active materials which shorten diffusion distance for lithium ions to react with superficial nanomaterials and intercalate inside CNT fabric nanocavities and act as Li ion reservoirs for Li/CNT-MnF_2 cell. However, larger MnF_2 loading than 70% inside CNT fabrics would decrease the unoccupied cavities and surfaces and weaken the interfaces between MnF_2 particles and CNT structure, which would decrease electrical connectivity inside the nanocomposite materials and would result in slow kinetics and accentuate the volume change effect during charge-discharge cycling. The preparation method used here helps to preserve the morphology, prevent segregation of phases and electrochemical disconnection, and prevent metal and F dissolution into the electrolyte.

4. Conclusion

In this work, CNT-MnF_2 nanocomposite fabrics were straightforwardly synthesized by surfactant-aided impregnation of $MnSiF_6$ inside acid-treated CNT fabrics followed by thermal decomposition of the precursor into MnF_2 and SiF_4 in Argon atmosphere at 400 °C for 4 h. The nanocomposites were characterized by XRD, SEM, TEM and EDS proving the infiltration of MnF_2 nanoparticles within acid-treated CNT fabric. The as prepared CNT-MnF_2 nanocomposite fabrics were tested as cathode material in Li-ion batteries. A specific capacity of 388 mAh/g at 0.1 C was measured for the CNT-MnF_2 nanocomposite fabric with 70% MnF_2 loading. Stable cyclability and almost 100% coulombic efficiency were achieved for these nanocomposite cathodes until 100 charge-discharge cycles. High specific capacities were retained at higher cycling rates (345 mAh/g at 0.2 C, 277 mAh/g at 0.5 C, 244 mAh/g at 1 C, 188 mAh/g at 2 C). Additionally, it is notable that MnF_2 loading affects largely the specific capacity of CNT-MnF_2 and MnF_2 loading between 70% and 80% led to the highest specific capacity. It can be concluded that tailoring the size of active materials infiltrated within conductive carbon matrices and assuring good connectivity between active materials and conductive supports can achieve excellent electrochemical properties (fast charge transfer and high rate performance) for MnF_2-based cathodes. This procedure can be generalized to other conversion-type cathode materials in order to develop flexible carbon-based materials with excellent cyclability and electrochemical performance that can be applied in portable electronic devices and integrated with renewable energy conversion systems.

Acknowledgments

This work was funded by a grant from the Qatar National Research Fund under its National Priorities Research Program award number NPRP7-567-2-216. Its contents are solely the responsibility of the authors and do not necessarily represent the official views of the Qatar National Research Fund. The authors are thankful to Prof Gleb Yushin from Georgia Institute of Technology for his collaboration in this subject.

References

[1] G. Jeong, Y.U. Kim, H. Kim, Y.J. Kim, H.J. Sohn, Prospective materials and applications for Li secondary batteries, Energy Environ. Sci. 4 (2011) 1986–2002.
[2] J. Li, M.C. Leu, R. Panat, J. Park, A hybrid three-dimensionally structured electrode for lithium-ion batteries via 3D printing, Mater. Des. 119 (2017) 417 424.
[3] F. Wu, G. Yushin, Conversion cathodes for rechargeable lithium and lithium-ion batteries, Energy Environ. Sci. 10 (2017) 435–459.
[4] G. Ali, J.H. Lee, W. Chang, B.W. Cho, H.G. Jung, K.W. Nam, K.Y. Chung, Lithium intercalation mechanism into $FeF_3 \cdot 0.5H_2O$ as a highly stable composite cathode material, Sci. Rep. 7 (2017), 42237. .
[5] G.G. Amatucci, N. Pereira, F. Badway, M. Sina, F. Cosandey, M. Ruotolo, C. Cao, Formation of lithium fluoride/metal nanocomposites for energy storage through solid state reduction of metal fluorides, J. Fluor. Chem. 132 (2011) 1086–1094.
[6] M. Sina, R. Thorpe, S. Rangan, N. Pereira, R.A. Bartynski, G.G. Amatucci, F. Cosandey, Investigation of SEI layer formation in conversion iron fluoride cathodes by combined STEM/EELS and XPS, J. Phys. Chem. C 119 (2015) 9762–9773.
[7] N. Kostoglou, I.E. Gunduz, T. Isik, V. Ortalan, G. Constantinides, A.G. Kontos, T. Steriotis, V. Ryzhkov, E. Bousser, A. Matthews, C. Doumanidis, C. Mitterer, C.

Rebholz, Novel combustion synthesis of carbon foam-aluminum fluoride nanocomposite materials, Mater. Des. 144 (2018) 222–228.
[8] S. Chong, Y. Chen, W. Yan, S. Guo, Q. Tan, Y. Wu, T. Jiang, Y. Liu, Suppressing capacity fading and voltage decay of Li-rich layered cathode material by a surface nano-protective layer of CoF_2 for lithium-ion batteries, J. Power Sources 332 (2016) 230–239.
[9] S. Kim, D. Seo, K. Kang, L. Wang, D. Su, J.J. Vajo, J. Wang, C. Link, F. Wang, S. Kim, D. Seo, K. Kang, L. Wang, D. Su, J.J. Vajo, Accessed ternary metal fluorides as high-energy cathodes with low cycling hysteresis, Nat. Commun. 6 (2018) 1–9.
[10] J. Li, S.H. Xu, S. Huang, L. Lu, L. Lan, S.H. Li, *In situ* synthesis of $Fe_{(1-x)}Co_xF_3$/MWCNT nanocomposites with excellent electrochemical performance for lithium-ion batteries, J. Mater. Sci. 53 (2017).
[11] M.F. Oszajca, K.V. Kravchyk, M. Walter, F. Krieg, M.I. Bodnarchuk, M.V. Kovalenko, Colloidal BiF_3 nanocrystals: a bottom-up approach to conversion-type Li-ion cathodes, Nano 7 (2015) 16601–16605.
[12] C.P. Guntlin, T. Zund, K.V. Kravchyk, M. Worle, M.I. Bodnarchuk, M.V. Kovalenko, Nanocrystalline FeF_3 and MF_2 (M: Fe, Co, and Mn) from metal trifluoroacetates and their Li(Na)-ion storage properties, J. Mater. Chem. A 5 (2017) 7383–7393.
[13] J. Li, F. Zhang, C. Wang, C. Shao, B. Li, Yi Li, Q.H. Wu, Y. Yang, Self nitrogen-doped carbon nanotubes as anode materials for high capacity and cycling stability lithium-ion batteries, Mater. Des. 133 (2017) 169–175.
[14] H. Kim, K. Lee, S. Kim, Y. Kim, Fluorination of free lithium residues on the surface of lithium nickel cobalt aluminum oxide cathode materials for lithium ion batteries, Mater. Des. 100 (2016) 175–179.
[15] H. Song, H. Cui, C.H. Wang, Extremely high-rate capacity and stable cycling of a highly ordered nanostructured carbon–FeF_2 battery cathode, J. Mater. Chem. A 3 (2015) 22377–22384.
[16] W. Gu, A. Magasinski, B. Zdyrko, G. Yushin, Metal fluorides nanoconfined in carbon nanopores as reversible high capacity cathodes for Li and Li-ion rechargeable batteries: FeF_2 as an example, Adv. Energy Mater. 5 (2015), 1401148. .
[17] V.A. Online, Y. Lu, Z. Wen, J. Jin, K. Rui, X. Wu, Hierarchical mesoporous iron-based fluoride with partially hollow structure: facile preparation and high performance as cathode material for rechargeable lithium ion batteries, Phys. Chem. Chem. Phys. 16 (2014) 8556–8562.
[18] J. Li, M.C. Leu, R. Panat, J. Park, A hybrid three-dimensionally structured electrode for lithium-ion batteries via 3D printing, Mater. Des. 119 (2017) 417–424.
[19] K. Rui, Z. Wen, Y. Lu, J. Jin, C. Shen, One-step solvothermal synthesis of nanostructured manganese fluoride as an anode for rechargeable lithium-ion batteries and insights into the conversion mechanism, Adv. Energy Mater. 5 (2015), 1401716. .
[20] H. Kim, K. Lee, S. Kim, Y. Kim, Fluorination of free lithium residues on the surface of lithium nickel cobalt aluminum oxide cathode materials for lithium ion batteries, Mater. Des. 100 (2016) 175–179.
[21] W. Chen, H. Zhang, X. Zhang, L. Wu, J. Liu, S.H. Liu, S.H. Zhong, Synthesis and electrochemical performance of carbon-coated $LiMnBO_3$ as cathode materials for lithium-ion batteries, Ionics 24 (2018) 73–81.
[22] F. Dou, L. Shi, P. Song, G. Chen, J. An, H. Liu, Dengsong Zhang, Design of orderly carbon coatings for SiO anodes promoted by TiO_2 toward high performance lithium-ion battery, Chem. Eng. J. 338 (2018) 488–495.
[23] X. Yao, G. Guo, P.-Z. Li, Z.-Z. Luo, Q. Yan, Y. Zhao, Scalable synthesis of honeycomblike V_2O_5/carbon nanotube networks as enhanced cathodes for lithium-ion batteries, ACS Appl. Mater. Interfaces 9 (2017) 42438–42443.
[24] X. Zhuang, P. Song, G. Chen, L. Shi, Y. Wu, X. Tao, H. Liu, D. Zhang, Coralloid-like nanostructured c-nSi/SiOx@cy anodes for high performance lithium ion battery, ACS Appl. Mater. Interfaces 9 (2017) 28464–28472.
[25] X. Fan, Y. Zhu, C.H. Luo, L. Suo, Y. Lin, T. Gao, K. Xu, C.H. Wang, Pomegranate-structured conversion-reaction cathode with a built-in li source for high-energy Li-ion batteries, ACS Nano 10 (2016) 5567−5577.
[26] M.J. Armstrong, A. Panneerselvam, C. O'Regan, M.A. Morrisab, J.D. Holmes, Supercritical-fluid synthesis of FeF_2 and CoF_2 Li-ion conversion materials, J. Mater. Chem. A 1 (2013) 10667–10676.
[27] S. Chong, Y. Chen, W. Yan, S. Guo, Q. Tan, Y. Wu, T. Jiang, Y. Liu, Suppressing capacity fading and voltage decay of Li-rich layered cathode material by a surface nano-protective layer of CoF_2 for lithium-ion batteries, J. Power Sources 332 (2016) 230–239.
[28] S.H. Tawa, T. Yamamoto, K. Matsumoto, R. Hagiwara, Iron(III) fluoride synthesized by a fluorolysis method and its electrochemical properties as a positive electrode material for lithium secondary batteries, J. Fluor. Chem. 184 (2016) 75–81.
[29] X. Fan, Y. Zhu, C. Luo, T. Gao, L. Suo, S.C. Liou, K. Xu, C.H. Wang, *In situ* lithiated FeF_3/C nanocomposite as high energy conversion reaction cathode for lithium-ion batteries, J. Power Sources 307 (2016) 435–442.
[30] X. Wang, W. Gu, J.T. Lee, N. Nitta, J. Benson, A. Magasinski, M.W. Schauer, G. Yushin, Carbon nanotube–CoF_2 multifunctional cathode for lithium ion batteries: effect of electrolyte on cycle stability, Small 11 (2015) 5164–5173.